

# Automatic Detection of Specular Reflections in Uterine Cervix Images

Gali Zimmerman-Moreno and Hayit Greenspan

Department of Biomedical Engineering, Tel-Aviv University, Tel-Aviv, Israel

## ABSTRACT

Specular reflections strongly affect the appearance of images, and usually hinder the computer vision algorithms applied to them. This is particularly the case with uterine cervix images. The highlights created by specular reflections are a major obstacle in the way of automatic segmentation of such images. We propose a method for the detection of specularities in cervix images that utilizes intensity, saturation and gradient information. A two-stage segmentation process is proposed for the identification of highlights. First, coarse regions that contain the reflections are defined. Second, probabilistic modeling and segmentation is used to achieve a precise segmentation inside the coarse regions. The resulting regions are filled by propagating the surrounding color information. The efficiency of the method for cervix images is demonstrated.

**Keywords:** Image quality, segmentation, statistical methods, specular reflections, highlights, cervigram, GMM, uterine cervix images.

## 1. INTRODUCTION

Specular reflections frequently appear in photographic images and interfere with numerous computer vision tasks, such as segmentation, object recognition, shape from shading and binocular stereo. Sometimes they provide useful information about the shape of the objects within the image. In all cases there is the need for identification and special treatment of these potentially problematic regions.

The focus of this work is on highlight (specularity) detection in a particular type of medical images, the cervigrams. Cervigrams are static photographic color images of the Uterine cervix obtained with a specialized 35-mm camera and a bright light source.<sup>1</sup> Cervicography is one of the methods for cervical cancer screening that uses visual testing based on the color change of cervix tissues when exposed to acetic acid.

The Cervix images used in this contribution were collected by the National Cancer Institute (NCI) during a longitudinal multi-year study carried out in Guanacaste, Costa Rica.<sup>2</sup> This work is part of an on-going effort towards the creation of automated cervigram analysis schemes. Segmentation methodologies are being developed for the identification of three main tissue types: the squamous epithelium (SE), which is smooth and pink, the columnar epithelium (CE) that appears red and irregular (textured) and the acetowhite (AW) region which is a transient, white-appearing epithelium following the application of acetic acid (Figure 1). Correct (highly sensitive and specific) identification of AW lesions is of clinical importance, since they are a major visual indicator in diagnostic tests for cervical cancer.<sup>3</sup>

Initial investigation into cervigram segmentation<sup>4</sup> revealed the significance of specular reflections elimination. Specular reflections (SR), or highlights, are generated in every cervigram as a consequence of the image acquisition process. They obstruct the tissues of interest thus hindering various stages of automatic segmentation. The bright white regions of SR may be mistaken for Aceto-White lesions which are usually relatively light. Furthermore, the high gradients created by SR amplify the local contrast causing erroneous results during extraction of texture features. Such miss-identification could cause an incorrect labeling of a cervigram. For example, the cervigram

---

Address all correspondence to H. Greenspan, E-mail: hayit@eng.tau.ac.il

Copyright 2006 Society of Photo-Optical Instrumentation Engineers. This paper will be published in SPIE Medical Imaging Symposium and is made available as an electronic reprint with permission of SPIE. One print or electronic copy may be made for personal use only. Systematic or multiple production, distribution to multiple locations via electronic or other means, duplications of any material in this paper for fee or commercial purpose, or modification of the content of the paper are prohibited

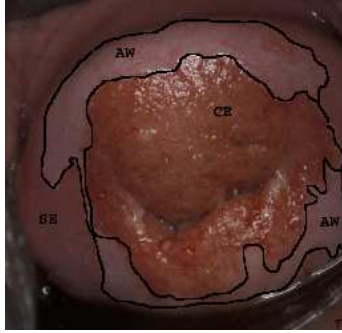


**Figure 1.** Three tissue types of interest marked on a cervigram.

in Figure 2(a) was marked by medical experts as untextured and AW-free. In this example the bright specular regions may be identified by an automated scheme as AW. Moreover, the high intensity gradients associated with SR (Figure 2(b)) create texture-like patterns on a tissue that is really smooth. Reliable identification of SR is therefore essential in order to facilitate automatic analysis and indexing of cervigrams.

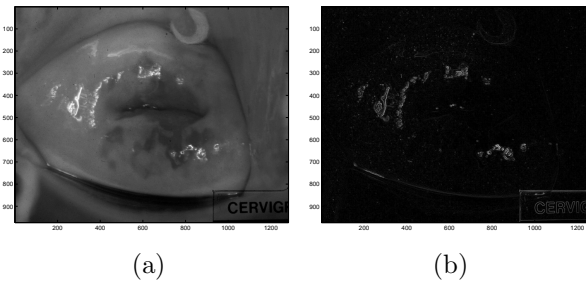


**Figure 2.** (a) Cervigram intensity image; (b) Magnitude of intensity gradient.

The subject of highlight elimination was extensively investigated in the last twenty years. Physics based approaches often utilize the Dichromatic Reflection Model (DRM) that describes a color of dielectric materials as a linear combination of an object color and highlight color. Klinker et al.<sup>5</sup> and Gershon et al.<sup>6</sup> devised automatic algorithms for highlights elimination, based on the DRM. They use the observation that the color histogram of an object with uniform diffuse color takes the shape of a skewed  $T$ . One limb of the  $T$  corresponds to purely diffuse points on the object while the second limb represents a highlight region. The proposed algorithms automatically identify the two limbs and use their directions to separate the diffuse and specular components of each pixel in this object. In this approach when the scene contains differently colored objects or object parts, the color clusters may overlap in 3D color space and the different  $T$ 's may become inseparable. Therefore, the image must be segmented in advance. On the other hand, the segmentation results are usually corrupted by highlights. In a later publication Klinker et al.<sup>7</sup> presented an algorithm that uses the DRM to generate an image segmentation along with descriptions of object and highlights.

Various later works use additional information in order to overcome some of DRM limitations. Nayar et al.<sup>8</sup> uses a polarization filter to determine the color of the specular component. Lin and Lee<sup>9</sup> propose a method based on integration of color and polarization information from multiple views. Uneyama and Godin<sup>10</sup> suggest an algorithm for separation of diffuse and specular components by use of polarization and statistical analysis. The use of an image sequence was proposed<sup>11</sup> for interpolating the color under the reflections.

The above approaches are not applicable to our case. Cervigram images include numerous similarly colored regions that differ in intensity and texture. In such a case we would expect the various  $T$ -shaped clusters to overlap. Furthermore, in the case of rough surfaces, the specular limb of a skewed  $T$  does not have a well defined direction.<sup>8</sup> This may be part of the reasons that the investigated images did not exhibit the skewed

$T$  behavior. Vogt et al.<sup>11</sup> also mentions the incompatibility of human tissues with the DRM. As for the use of additional information, such as polarization measurements or multiple images, this information is not available in the present research.

Several works handle the problem of SR based on a single image without assuming a physics based model. Groger et al.<sup>12</sup> propose to segment specular reflections on a heart surface by a simple threshold on the gray scale image. They present two reconstruction schemes for the SR pixels, that are based on the surrounding information: linear interpolation between boundary pixels and anisotropic diffusion. Torres et al.<sup>13</sup> introduce a scheme for automatic detection of highlights using a two-dimensional intensity and saturation histogram of an image that underwent contrast stretching. It is suggested that all of the SR pixels are located in a well defined region, so that the highlights may be segmented by marking all the pixels in this region.

A small number of works addresses the problem of specularities in cervical images. A semi-automated algorithm is introduced in a work by Hervet and Kardouchi.<sup>14</sup> An image is first segmented into a large number of regions. The user is required to manually identify the segments belonging to specularities. A histogram transform is then applied between the highlight and the normal tissue region thus eliminating the highlights. In another work, Van Raad<sup>15</sup> models the pixel distribution in an image as a Gaussian Mixture Model in RGB color-space, where one Gaussian represents SR pixels and another one represents the rest of the image. This model is created based on a set of images. A linear distance measure is used to classify pixels in an image to SR and non-SR pixels.

The experiments conducted during the current investigation show that the learning of global models or thresholds, as required in the above works,<sup>12,13,15</sup> is problematic due to the large variation in the appearance and characteristics of the cervix images. The deviations in the visual appearance of cervigrams are evident in the images that are shown throughout this paper.

In this contribution an adaptive unsupervised approach is proposed that is flexible enough for the entire variety of the images within the cervigram archive. The aim here is to reliably identify the specular reflections in cervix images, thus facilitating further computerized processing of these images. For instance, specular regions are to be discarded when color-based image segmentation is performed so that they are not mistaken for AW. On the other hand, when extracting texture measures, the specular regions have to be not only identified, but completely eliminated. For this purpose a simple filling in scheme is proposed, that removes the strong gradients associated with SR, but does not over-smooth the original texture in the image.

We propose an algorithm for automatic unsupervised detection and elimination of specular reflections, which receives a single image as an input. Gradient information is utilized in conjunction with hue and saturation in order to minimize the occurrence of false positives. First, candidate SR regions, which contain all of the specularities as well as some additional pixels are defined. The distribution of pixels within these regions is automatically modeled as a mixture of Gaussians in a defined feature space, and probabilistic segmentation is performed. The resulting regions are filled by propagating color information from the surrounding non-SR regions.

A detailed description of the algorithm is presented in section 2. Results of the algorithm and validation experiments are shown in section 3. Section 4 summarizes the work.

## 2. SEGMENTATION OF THE REFLECTION REGIONS

Specular Reflections appear as small and bright regions in various parts of the cervigram. Their modeling and segmentation is a difficult task, due to extreme class imbalance - the number of pixels belonging to SR regions is small relatively to the number of all the pixels in the image. Thus, SR pixels tend to be affiliated with other clusters, rather than being recognized as a separate cluster. In particular, there is an overlap between SR and acetowhite regions in color-space, i.e some of the AW regions are so light that they may be erroneously marked as specularities.

In order to overcome these difficulties, the proposed scheme starts with focusing the analysis into automatically defined regions of interest, the so-called candidate SR regions. Inside of these regions the classes are more balanced and correct pixel classification is possible.

## 2.1. Identification of the candidate regions

Candidate SR regions are coarse regions in which the highlights are most likely to be found. Specularities always have very intense brightness ( $I$ ) and low color saturation ( $S$ ) values.<sup>16</sup> This observation allows the definition of initial regions of interest, by applying thresholds on  $S$  and  $I$  of the image pixels. Intensity and Saturation are defined as follows:

$$I = \frac{R + G + B}{3} \quad (1)$$

$$S = 1 - \frac{\min(R, G, B)}{I} \quad (2)$$

and a set of thresholds are loosely selected (motivated by<sup>16</sup>):

$$I > 0.4 \cdot I_{max}, S < 0.6 \cdot S_{max} \quad (3)$$

where  $I_{max}$  and  $S_{max}$  are the maximum intensity and saturation in the image respectively. Following the thresholding process, all of the SR are contained inside these coarse regions of interest.

In images containing moist tissues, such as cervigrams, reflection regions appear as small bright spots and therefore are associated with high gradients in their vicinity. This allows further refining of the candidate regions by selecting only the pixels in the vicinity of high gradients (a 10 pixel neighborhood is used). Regions of strong gradients were located by applying a threshold on the magnitude of the intensity gradient:

$$|\nabla G| = \sqrt{\left(\frac{\partial I}{\partial x}\right)^2 + \left(\frac{\partial I}{\partial y}\right)^2} > 0.15 \quad (4)$$

The resulting regions contain all of the SR pixels, as well as some additional neighboring pixels, approximately in equal proportion (Figure 3(b)). The above set of thresholds was found empirically through a detailed study of a large database of cervigrams. Other types of images may require a different set of thresholds.

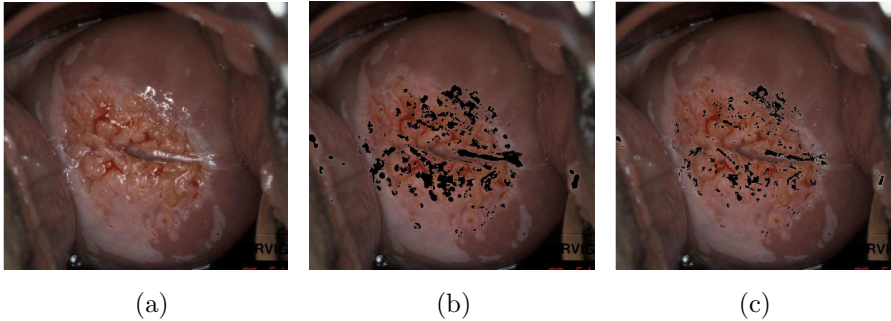


**Figure 3.** SR Identification: (a) Original cervigram (cropped); (b) Candidate SR regions are marked in black; (c) Final identification of SR (black).

## 2.2. Statistical modeling and segmentation of SR

The precise extraction of highlights from the previously defined coarse regions is performed next. The pixels within the candidate regions are mapped into a two dimensional  $S - V$  feature space, where  $S$  and  $V$  are Saturation and Value of the standard HSV color space.<sup>17</sup> Experiments indicate that the hue characteristic of the pixels does not contribute to SR detection, and is therefore ignored. Each pixel is represented with a two-dimensional vector. Pixels are grouped into homogeneous regions by grouping the feature vectors in the selected  $S - V$  feature space. Each homogeneous region in the image plane is thus represented by a Gaussian distribution, and the set of regions in the image is represented by a Gaussian mixture model.

The distribution of a  $d$ -dimensional random variable is a mixture of  $k$  Gaussians if its density function is :

$$f(x) = \sum_{j=1}^k \alpha_j \frac{1}{\sqrt{(2\pi)^d |\Sigma_j|}} \exp\left\{-\frac{1}{2}(x - \mu_j)^T \Sigma_j^{-1} (x - \mu_j)\right\}, \quad (5)$$

where  $d$  is the feature space dimension,  $\alpha_j$  are the probabilities of the occurrence of each Gaussian, and  $\mu_j, \Sigma_j$  are the mean and the covariance matrix of each Gaussian cluster respectively. The Expectation-Maximization (EM) algorithm,<sup>18</sup> is used to determine the maximum likelihood parameters of a mixture of Gaussians in the selected feature space.

An immediate transition is possible between GMM representation and probabilistic tissue segmentation. The labelling of a pixel related to the two-dimensional feature vector  $x$  is chosen as the maximum *a posteriori* probability:

$$label(x) = \arg \max_j \alpha_j f(x | \mu_j, \Sigma_j) \quad (6)$$

i.e. each pixel gets affiliated with the most probable Gaussian cluster in the learned GMM.

Experiments conducted in the current study reveal that SR pixels are best modeled by two Gaussians. One represents the brightest, almost white pixels, that have lost most of their chromatic information. The other Gaussian represents the less bright pixels that retain some of their original color. The non-SR regions are modeled by two additional Gaussians to account for various tissue types. An overall mixture of 4 Gaussians is used to model the candidate regions. Following the modeling stage pixels corresponding to the two Gaussians with the highest mean intensity are selected as the SR pixels. Figure 3(c) shows the final SR labeled pixels (black) following the statistical modeling and segmentation.

### 2.3. Elimination of the reflections: filling in the missing pixels

A simple filling scheme is proposed, which eliminates the strong gradients associated with the SR, while preserving the original texture. This is important in particular for further region analysis, such as extraction of texture features. Based on the observation that the highlights formed on the moist surface of the cervix are very small, a simplifying assumption is made, that the color underneath each highlight is nearly constant and similar to the color of the pixels in the immediate surroundings.

The color information of the surrounding pixels is propagated into the specular regions, thus creating a smooth filling of the image. First, the color values of the detected SR pixels are set to zero. An iterative process follows in which each pixel inside the SR region is assigned the mean color of its non-zero neighbors. The process is described in pseudocode below. Let  $SR$  be the set of all the pixels that were marked as specular in the previous step and let  $(i, j)$  denote an index of an image pixel.

1. for all  $(i, j) \in SR$  set  $(R, G, B)_{i,j} = (0, 0, 0)$
2. while  $SR \neq \emptyset$
3. for all  $(i, j) \in SR$ :
4.  $(R, G, B)_{(i,j)} = \frac{1}{N_{nz}} \sum_{(m,n) \in nz} (R, G, B)_{m,n}$  where  $(R, G, B)_{i,j}$  is the color of a pixel  $(i, j)$ ,  $nz$  is the set of all non zero neighbors of the pixel  $(i, j)$ , and  $N_{nz}$  is the number of these non-zero neighbors.
5. end for
6. update the  $SR$  set:  $SR = \{(i, j) \mid (R, G, B)_{i,j} \neq (0, 0, 0)\}$
7. end while

In the first iteration, each SR pixel that is adjacent to the SR region boundary is assigned the mean color of its non-zero neighbors. The pixels that were assigned non-zero values in the first iteration are used in the following iteration for assigning color to the pixels farther from the boundary. This step is repeated until the entire SR region is filled. The process is computationally feasible due to the small size of a typical highlight. Several results of the filling scheme are presented in section 3, Figure 4.

**Table 1.** Grading statistics for detection and filling

grade	detection	filling
1	103 (85.8 %)	71 (59%)
2	4 (3.3%)	18 (15%)
3	13 (10.8%)	31 (25.8%)
4	0	-
5	0	-

### 3. RESULTS

The proposed algorithm was tested on a large set (several hundreds) of cervix images provided by National Cancer Institute (NCI), National Institutes of Health (NIH).

When evaluating the algorithm performance, we consider two main aspects: detection quality and filling quality. It should be noted that it is difficult to quantitatively evaluate the results since all of the images were taken in an unsupervised environment and there are no ground truth highlight-free images available. Precise manual segmentation of all of the specularities in a Cervigram is tedious and time consuming as there are hundreds of SR spots in each Cervigram, some of them very small. Furthermore, manual segmentation results are highly dependent on the individual marking style of the human expert. Therefore it is impossible to obtain enough precise manual segmentations by enough experts in order to enable a reliable quantitative validation. However, a subjective quality grading was conducted with the cooperation of a medical expert on a set of 120 images. The expert was shown two results for each cervigram: one is an image with the SR marked in black, and another is the filled in image with the highlights eliminated. He was requested to grade the detection quality on the scale of 1 to 5, where 1 is the best possible detection and 5 is the worst. The filled image was graded on a scale of 1 to 3, here the grade 3 means low filling quality. Several results, as presented to the expert are shown in Figure 4 along with their gradings. The gradings for all of the 120 images are summarized in Table 1. For example, out of 120 images, the detection grade is 1 for 103 images, which constitutes 85.8% of the images.

In order to further assess the filling quality we consider the effect of SR elimination on intensity gradients in the image. As stated earlier in this paper, the strong gradients introduced by specularities interfere with the extraction of texture features that may be necessary during automatic analysis of Cervigrams. Therefore it is vital that the filling scheme attenuates the effect of specularities on the gradients in the image. Figure 5 presents gradient maps before and after SR filling. Intensity gradients in original images are shown in column (b) and the gradients in the filled images are in column (d). As seen from Figure 5, most of the gradients that arise from SR are indeed eliminated by the filling process. For example in the image of second line, the SR are located on relatively smooth epithelium. The gradient map of this image (b), contains strong gradients arising from specularities. These gradients are successfully eliminated, as shown in the gradient map of the filled image (d). Example(1) of Figure 5 presents a different situation. In its upper portion, the specularities appear on a rough textured tissue. The gradients arising from the tissue roughness are amplified by SR, as can be observed in the corresponding gradient map (b). After SR elimination the gradient map (d), still exhibits the gradients arising from the tissue roughness, but without the amplification of specularities, and the texture pattern is preserved.

### 4. DISCUSSION

We have described and tested a fully automatic method for detection and elimination of specular reflections in cervigram images. The purpose of the suggested process is mainly to prepare the cervigrams for further automated analysis, which is usually hindered by the presence of specular reflections. The desired results are clear identification of specular regions, and the so called filled image. The proposed algorithm was tested on a large set of images (a subset of which was presented) and was shown to achieve good results.

Detection was found visually satisfying by medical experts. This follows from the fact that 90% of the cases were graded as very high quality (grades 1, 2 on a scale of 1 to 5). As for the filling, it is less reliable. This

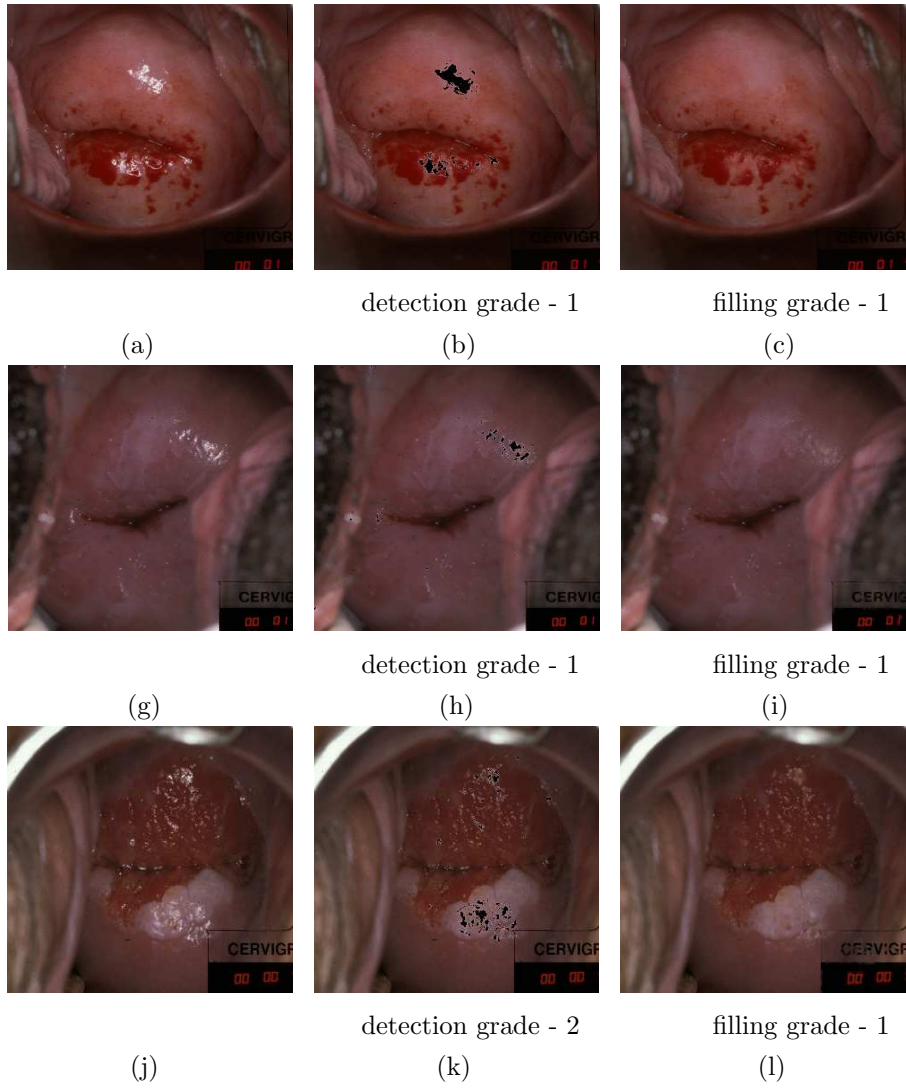


**Figure 4.** Results and their gradings by expert: Original cervigrams (cropped) - left column; Identification of SR (black) - middle column; Filled in images - right column.

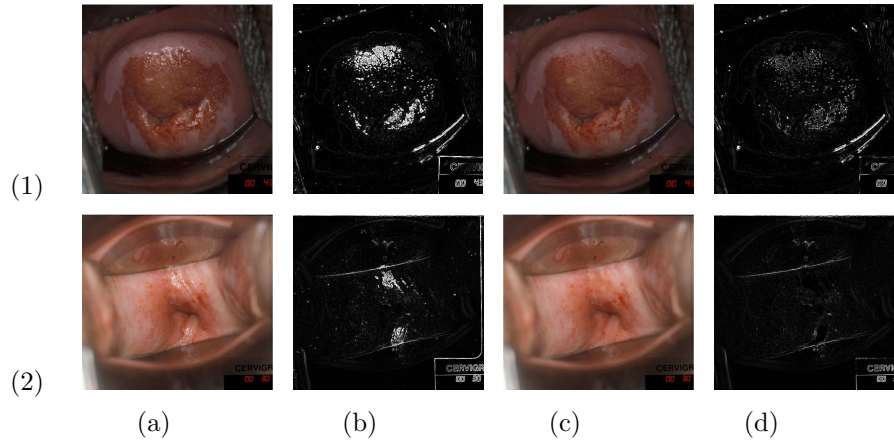


**Figure 5.** Specular Reflections elimination and the effect on gradients: (a) original cervigrams (cropped); (b) intensity gradients in original image; (c) cervigrams after SR elimination (detection and filling); (d) intensity gradients in filled images (after detection and filling).

is to be expected, since the filling method relies in the surrounding non-specular pixels and does not attempt to recover the real color beneath the specularities. However, as stated before, the main purpose of the filling procedure was the reduction of the strong gradients associated with the SR, while preserving the original texture. This is achieved as shown in the results section.

The main limitation of the algorithm arises from hard definition of the number of Gaussians when segmenting the initial SR regions. The selected model ( $K = 4$  Gaussians, 2 are affiliated with SR) was chosen as optimal for large number of cervigrams. However, adaptive selection of the  $K$  parameter for each image will make the procedure more robust, and is part of our future work.

The presented method was developed and optimized specifically for Cervigram images that contain moist rough tissues, and is not intended for smooth and almost mate objects. Other possible applications are various medical images containing moist live tissues, such as endoscopic or heart surface images.

#### Acknowledgement

We would like to thank the Communications Engineering Branch, National Library of Medicine, NIH, for the data and support of the work.

We would especially like to thank Jose Jeronimo M.D., National Cancer Institute, for the evaluation of the algorithm performance.

## REFERENCES

1. Ferris, D.G., Schiffman, M., Litaker, M.S.: Cervicography for triage of women with mildly abnormal cervical cytology results. *American Journal Obstetrics and Gynecology* **185** (2001) 939–43
2. Herrero, R., Schiffman, M.H., Bratti, C., Hildesheim, A., Balmaceda, I., Sherman, M.E., Greenberg, M., Cardenas, F., Gomez, V., Helgesen, K., Morales, J., Hutchinson, M., Mango, L., Alfaro, M., Potischman, N.W., Wacholder, S., Swanson, C., Brinton, L.A.: Design and methods of a population-based natural history study of cervical neoplasia in a rural province of costa rica: the guanacaste project. *Pan American Journal of Public Health* **1** (1997) 362–375
3. Pogue, B.W., Kaufman, H.B., Zelenchuk, A., Harper, W., Burke, G.C., Burke, E.E., Harper, D.M.: Analysis of acetic acid-induced whitening of high-grade squamous intraepithelial lesions. *Journal of Biomedical Optics* **6** (2001) 397–403
4. Gordon, S., Zimmerman, G., Greenspan, H.: Image segmentation of uterine cervix images for indexing in PACS. In: *Proc. of 17th IEEE Symposium on Computer-Based Medical Systems*. (2004) 298–303

5. Klinker, G., Shafer, S.A., Kanade, T.: The measurement of highlights in color images. *International Journal of Computer Vision* **2** (1988) 7–32
6. Gershon, R., Jepson, A.D., Tsotsos, J.K.: Highlight identification using chromatic information. In: *Proceedings of the first International Conference on Computer Vision (ICCV)*. (1987) 161–171
7. Klinker, G., Shafer, S.A., Kanade, T.: A physical approach to color image understanding. *International Journal of Computer Vision* **4** (1990) 7–38
8. Nayar, S.K., Fang, X.S., Boulton, T.: Removal of specularities using color and polarization. In: *Proceedings 1993 IEEE Computer Society Conference on Computer Vision and Pattern Recognition*. IEEE Comput. Soc. Press., Los Alamitos, CA (1993) 583–590
9. Lin, S., Lee, S.W.: Detection of specularity using stereo in color and polarization space. *Computer Vision and Image Understanding* **65** (1997) 336–346
10. Uneyama, S., Godin, G.: Separation of diffuse and specular components of surface reflection by use of polarization and statistical analysis of images. *IEEE Transactions on Pattern Analysis and Machine Intelligence* **26** (2004)
11. Vogt, F., Paulus, D., Heigl, B., Vogelgsang, C., Neimann, H., Greiner, G., Schick, C.: Making the invisible visible: Highlight substitution by color light fields. In: *First european conference In Color Graphics, Imaging and Vision*, Poitiers, France (2002) 352–357
12. Groeger, M., Sepp, W., Ortmaier, T., Hirzinger, G.: Reconstruction of image structure in presence of specular reflections. In: *Pattern Recognition, 23rd DAGM Symposium*. Volume 2191 of LNCS., Munich, Germany (2001) 53–60
13. Torres, F., Angulo, J., Ortiz, F.: Automatic detection of specular reflectance in colour images using the ms diagram. In: *CAIP03*. (2003) 132–139
14. Hervet, E., Kardouchi, M.: Segmentation and histogram transform of color colposcopic images. In: *International Conference on Signal and Image Processing (ICISP)*. Volume 2., Agadir, Morocco (2003) 412–420
15. Van-Raad, V.: Frequency space analysis of cervical images using short time fourier transform. in *Proceedings of the IASTED International Conference of Biomedical Engineering* **1** (2003) 77–81
16. Lehmann, T.M., Palm, C.: Color line search for illuminant estimation in real-world scenes. *Optical Society of America* **18** (2001) 2679–2691
17. Smith, A.R.: Color gamut transform pairs. In: *International Conference on Computer Graphics and Interactive Techniques, Proceedings of the 5th annual conference on Computer graphics and interactive techniques*. (1978) 12 – 19
18. Greenspan, H., Goldberger, J., Ridel, L.: A continuous probabilistic framework for image matching. *Journal of Computer Vision and Image Understanding* **84** (2001) 384–406